Lenalidomide stabilizes protein-protein complexes by turning labile intermolecular H-bonds into robust interactions.

Marina Miñarro-Lleonar,[1,2,3] Andrea Bertran-Mostazo[1, 3], Jorge Duro,[1,2] Xavier Barril,[1,2,3,4] Jordi Juárez-Jiménez,[1,2]**

[1]Unitat de Fisicoquímica, Departament de Farmàcia i Tecnologia Farmacéutica, i Fisicoquímica. Facultat de Farmacia I Ciències de l'Alimentació. Universitat de Barcelona (UB). Av. Joan XXIII, 27-31, 08028 Barcelona, Spain.

[2]Institut de Química Teòrica i Computacional (IQTC), Universitat de Barcelona (UB), Barcelona, Spain.

[3]Institut de Biomedicina, Universitat de Barcelona (UB), Barcelona, Spain

[4] Catalan Institution for Research and Advanced Studies (ICREA), Barcelona 08010, Spain.

Abstract

Targeted protein degradation (TPD) is emerging as a very promising strategy to modulate protein activities in several diseases, spearheaded by anti–myeloma drugs lenalidomide and pomalidomide. It has been recently demonstrated that the mechanism of action of these drugs involves the increased degradation of several proteins, including the transcription factors Ikaros and Aiolos as well as the enzyme Caseine Kinase 1α (CK1α). It has been shown that lenalidomide and pomalidomide are able to stabilize the complex between the E3 ligase Cereblon ($CRL4^{CRBN}$) and the aforementioned proteins, while, remarkably, the stability of the protein-protein interaction is very low. Even though the structures for these complexes have

been determined, there are no evident interactions that can account for the high formation efficiency of the ternary complex. In this work, we have leveraged Molecular Dynamics to shed light into the molecular determinants underlying the stabilization effect exerted by lenalidomide in the complex between $CRL4^{CRBN}$ and CK1α. Furthermore, we evaluated the effect that different mutations of CK1α in the stability of the ternary complex $CRL4^{CRBN}$–lenalidomide–CK1α and provide a thermodynamic and kinetic rational for the stabilization effect. These results pave the way to further understand cooperativity effects in drug–induced protein–protein complexes and could help in the future design of improved targeted molecular degraders.

Introduction

The concept of molecular glues (MGs) was introduced by Zheng and co–workers[1] to describe the stabilizing effect of the plant hormone auxin on several complexes with the SCF^{TIR1} ubiquitin ligase complex. Subsequently, it has been revealed that this mechanism is quite common in nature[2–5] and that even a number of widely used drugs such as the immunosuppressant drug Cyclosporin A[6] or the anti–cancer agents Paclitaxel[7] or Indisulam[8] share a similar mechanism of action. These findings have spured interest in leveraging selective stabilization of protein–protein interaction in drug discovery. However, it has been repeatedly noted in the literature[9–11] that MGs discovery is too reliant on serendipity and that the future development of successful MGs as therapeutic agents ought to shift into more rational approaches and further understanding of the molecular mechanisms underpinning the ligand–induced stabilization of protein–protein interactions. Contrary to traditional drug discovery, which focuses on the formation of binary complexes, rational development of MGs will require detailed understanding of the formation of ternary complexes, which often imply non–additive mechanisms.[12] The physicochemical factors underlying these mechanisms are usually difficult to anticipate from structural analysis or common Computer Aided Drug Design protocols such

as docking or Virtual Screening.[3] Nonetheless, they are critical to the selective stabilization of protein–protein complexes, and must be understood to fully exploit the therapeutic opportunities offered by MGs.

A landmark example of the potential of MGs to impact human health is provided by thalidomide derivatives lenalidomide and pomalidomide, so called IMiDs, widely used in the treatment of multiple myeloma. Only recently it was described that these molecules induce the ubiquitination and degradation of the transcription factors Ikaros (IKZF1) and Aiolos (IKZF3)[13] and the enzyme Casein Kinase 1α (CK1α)[14] by stabilizing the complex of these proteins with the E3 ligase CRBN, which is the substrate receptor of the CUL4–RBX1–DDB1 ubiquitin ligase complex (CRL4). IMiDs are accommodated in a tryptophan cage in the substrate binding domain of CRBN[15] and structural evidence has shown that IKZF1,[16] CK1α[17] and other proteins[18] bind to the CRBN–IMiD interface, establishing a set of protein–protein interactions through a β–hairpin loop structure that contains a Gly residue on the apex.[5,16,17] In a recent work, Cao et. al.[19] estimated that pomalidomide stabilizes the IKZF1–CRBN complex by around fourfold, while lenalidomide stabilizes the CK1α–CRBN complex by around 30–fold. The authors also proposed that instead of creating new sets of interactions, MGs in general, and IMiDs in particular, must be able to stabilize pre–existing protein–protein interactions. Analysis of the structural data available seems to support this hypothesis, as the direct intermolecular interaction between lenalidomide–CK1α[17] and pomalidomide–IKZF1[16] are rather unremarkable and thus, cannot account for the increase in stability of the ternary complex. These observations highlight the importance of the non–additive mechanism at play in these interactions.[12] In this work, we use biomolecular simulations to evidence that the stabilization effect exerted by lenalidomide in the complex between CRBN and CK1α relies on the its ability to increase the structural stability of three key H–bonds at the CRBN–CK1α interface. Using data for four different mutants of CK1α we demonstrate that the robustness of

these three H–bonds directly correlates with the stability of the ternary CRBN–lenalidomide–CK1α complex, even when mutations do not directly disturb the ability of either protein to establish these interactions. The underlying mechanism is proposed to depend on the capacity of lenalidomide to provide hydrophobic shielding to pre–existing protein–protein hydrogen bonds, thus increasing the structural, kinetic and thermodynamic stability of the complex. We anticipate that this may be a general mechanism that can be exploited for the future rational development of MG.

Results

Presence of lenalidomide results in stronger H–bond interactions at the CRBN–CK1α interface.

Examination of the protein–protein interface of the CRBN–lenalidomide–CK1α complex reveals that there are three protein–protein hydrogen bonds between the 36–42 β–hairpin loop of CK1α and the C–terminal domain of CRBN (Supplementary Figure S1). Namely, the side–chains of CRBN residues Asn351, His357 and Trp400 engage the backbone carbonyl oxygens of the CK1α residues Ile37, Thr38 and Asn39 respectively. These interactions hereafter referred to as $CRBN^{Asn351}$–$CK1\alpha^{Ile37}$, $CRBN^{His357}$–$CK1\alpha^{Thr38}$ and $CRBN^{Trp400}$–$CK1\alpha^{Asn39}$ respectively, have been demonstrated to be key for the recruitment of CK1α by CRBN.[17] However, there is no evident factor precluding the formation of these interactions in the absence of lenalidomide, which is in line with the hypothesis of stabilization of pre–existing protein–protein complexes put forward by Cao and co–workers. Previous works have shown that most stable receptor–ligand complexes display, at least, one robust and hard–to break intermolecular H–bond,[20–22] and the importance of these interactions has also been highlighted as a main player in protein structural stability.[23,24] Therefore, we investigated the energetic cost

of independently breaking each of the H–bonds identified at the CRBN–CK1α interface (Figure 1) combining Steered Molecular Dynamics and the Jarzynski's equality.[25,26]

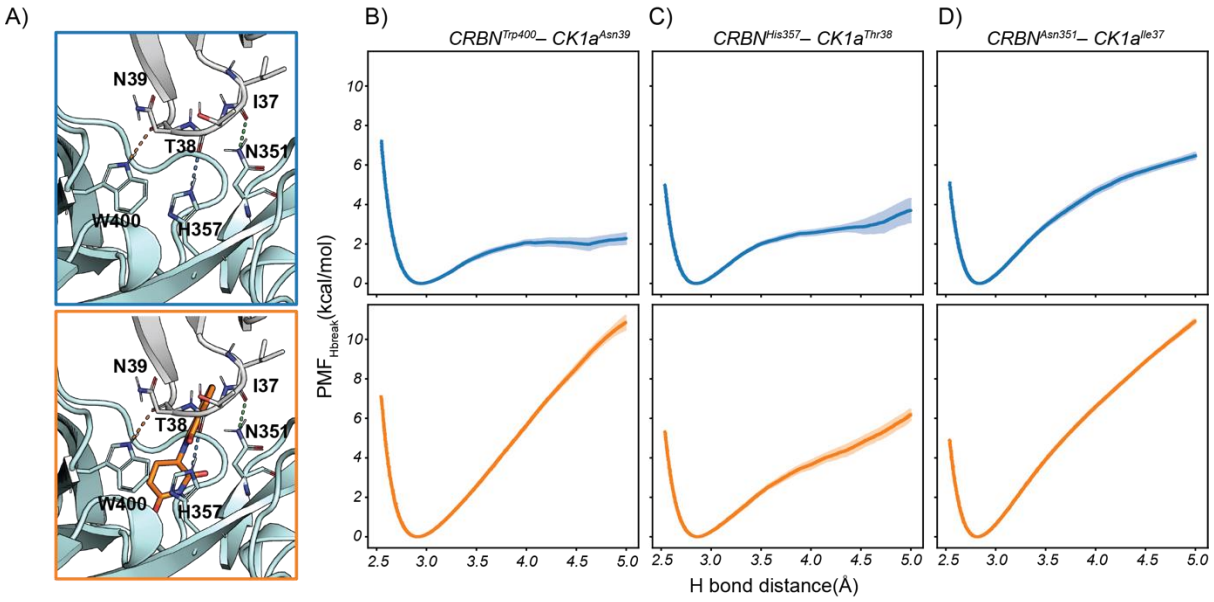

Figure 1: H–bond dissociation energy profiles in the presence and absence of lenalidomide at the CRBN–CK1α interface. **A**. Detailed view of the CK1α–CRBN dimeric interface (top) and its ternary complex with lenalidomide (bottom). **B.** Energy profile of the CRBN^{Trp400}– CK1α^{Asn39} H–bond in the absence (top) and presence (bottom) of lenalidomide. **C.** Energy profile of the CRBN^{His357} – CK1α^{Thr38} H–bond in the absence (top) and presence (bottom) of lenalidomide. **D.** Energy profile of the CRBN^{Asn351} – CK1α^{Ile37} H–bond in the absence (top) and presence (bottom) of lenalidomide.

Although convergence of sampling is usually a concern when applying the Jarzynski relationship, we consider that the reduced number of degrees of freedom that the system may access during sampling of the rupture of a given H–bond (where donor and acceptor are pulled apart from 2.5 Å to 5 Å, *vide infra*) will allow to calculate Potentials of Mean Force along the separation distance between donor and acceptor (hereafter referred to as PMF of H–bond breakage or PMF$_{HB_break}$) of sufficient accuracy as to distinguish strong from weak H–bond interactions, similarly to what us and others have previously reported in the literature for other systems.[21,27,28] By comparing the values of PMF$_{HB_break}$, we established that, in the absence of lenalidomide, the stronger H–bond is CRBN^{Asn351}–CK1α^{Ile37} (PMF$_{HB_break}$ = 6.4 +/- 0.1

kcal/mol) followed by the CRBN^{His357}–CK1α^{Thr38} interaction (PMF_{HB_break} = 3.7 +/- 0.6 kcal/mol) and the CRBN^{Trp400}–CK1α^{Asn39} interaction (PMF_{HB_break} = 2.3 +/- 0.3 kcal/mol). The presence of lenalidomide at the interface causes a large increase in the energy necessary to break the three H–bonds, with estimated PMF_{HB_break} of 10.9 +/- 0.1, 6.3 +/- 0.3 and 11.0 +/- 0.4 kcal/mol for the CRBN^{Asn351}–CK1α^{Ile37}, CRBN^{His357}–CK1α^{Thr38} and CRBN^{Trp400}–CK1α^{Asn39} interactions respectively (Table 1). We examined the 3D–structure of the ternary complex to obtain clues about the stabilization of the investigated H–bonds. The only direct H–bond between lenalidomide and CRBN (the carbonyl group of the oxoisoindol moiety with the side–chain of Asn351) is insufficiently connected to the protein–protein H–bonds to suggest that it can cause a concerted change in the interaction network. Instead, the increased stability may be explained by the change of local environment around the H–bonds. Indeed, it has been previously shown that incoming water molecules catalyze the rupture of solvent exposed H–bonds, by decreasing the energetic barrier required to bring apart donor and acceptor.[20,29] Based on these observations, we hypothesized that the main role of lenalidomide will be to create a hydrophobic environment around the protein–protein interface that effectively shields the H–bonds from incoming water molecules.

Reinforced H–bonds display increased hydrophobic shielding at the CRBN–CK1α interface.

To probe our hypothesis that lenalidomide stabilizes the CRBN–CK1α complex mainly by hydrophobic shielding effects, we studied the changes on the local environment of the three key H–bonds at the interface upon binding of the MG. The radial distribution function (RDF) provides the average number of water molecules found around a certain atom with respect to what would be expected on the bulk solvent during the course of a Molecular Dynamics simulation.

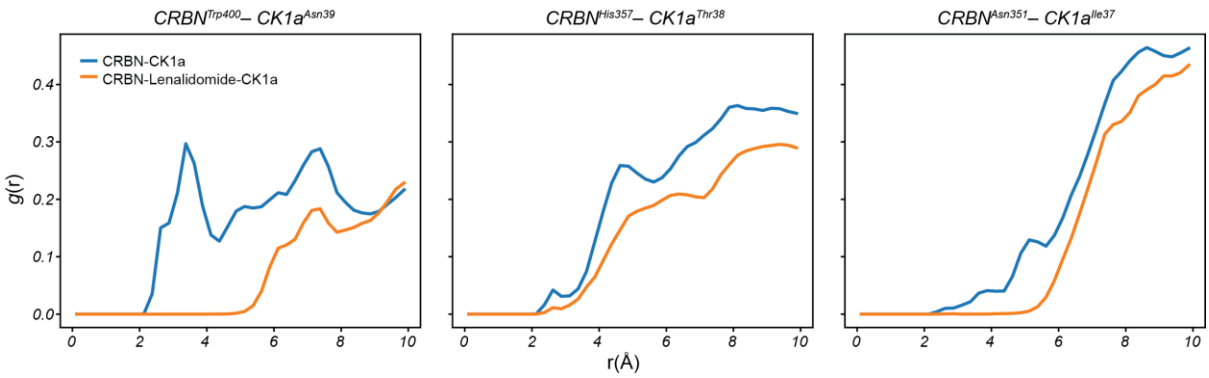

Figure 2: Radial Distribution Function (RDF) of water molecules around the backbone carbonyl oxygen of CK1α involved on the key CRBN–CK1α H–bonds. The blue line represents values for the two–body complex CRBN–CK1α and the orange represents values for the three–body complex CRBN–lenalidomide–CK1α

Therefore, it can be used as a proxy to estimate the solvent exposure of certain atoms or residues. We determined the RDF of the backbone carbonyl groups of CK1α in molecular dynamics of both the CRBN–CK1α and CRBN–lenalidomide–CK1α complexes (Figure 2) in which the H–bond distances for the three key interactions was kept between 2.5 and 3.5 Å using flat bottom restraints (see the methods section for further details). As expected for atoms at the interface of the protein–protein complex, their water exposure is relatively low. However, there was a noticeable reduction on the RDF around the backbone carbonyl of Asn39 (from 0.3 in the binary complex to 0 in the ternary complex). Furthermore, the RDF around the $CRBN^{Asn351}$ – $CK1\alpha^{Ile37}$ and the $CRBN^{Trp400}$– $CK1\alpha^{Asn39}$ H–bonds for radii below 5 Å drops to 0 in the presence of lenalidomide. On the other hand, the reductions in the RDF for the $CRBN^{His357}$ – $CK1\alpha^{Thr38}$ H–bond – the interaction that is least reinforced by the presence of lenalidomide – is relatively minor.

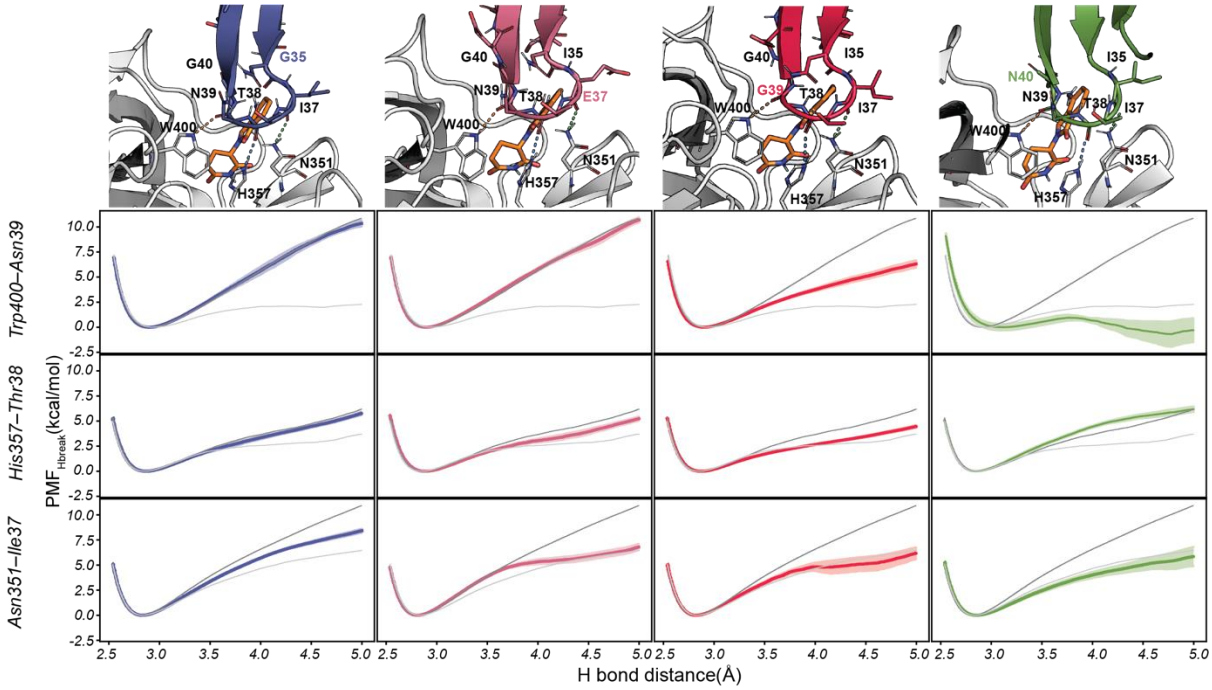

Figure 3: H–bond dissociation energy profiles in the presence and absence of lenalidomide at the CRBN–CK1α interface. Detailed view of the CRBN–lenalidomide–CK1α interface for ^{I35G}CK1α, ^{I37E}CK1α, ^{N39G}CK1α and ^{G40N}CK1α and associated PMF_{HB_break} profiles for CRBN^{Trp400}–CK1α^{Asn39} (Top), CRBN^{His357}–CK1α^{Thr38} (middle) and CRBN^{Asn351}–CK1α^{Ile37} (bottom). PMF_{HB_break} profiles for CRBN–lenalidomide–^{wt}CK1α (dark grey) and the CRBN–^{wt}CK1α (light grey) are included for reference

H–bond robustness correlates with the measured stability of CRBN–lenalidomide–^{MUT}CK1α complexes.

Petzold et. al. reported that the ternary complexes between CRBN–lenalidomide and CK1α mutants ^{I35G}CK1α, ^{I37E}CK1α, ^{N39G}CK1α and ^{G40N}CK1α displayed decreasing stability.[17] We therefore investigated whether the robustness of the H–bonds at the interface on these ternary complexes was diminished with respect to the CRBN–lenalidomide–CK1α complex (Figure 3 and Table 1).

Analysis of the energetic profiles of H–bond breakage showed that ^{N39G}CK1α and ^{G40N}CK1α displayed the greatest alterations, both with ΔPMF_{HB_break} in excess of 4 kcal/mol for the

CRBN^{Asn351}–CK1α^{Ile37} and CRBN^{Trp400}–CK1α^{Asn39} interactions. In the case of the CRBN^{His357}–CK1α^{Thr38} interaction, there was a lesser reduction in ^{N39G}CK1α (ΔPMF_{HB_break} = 1.7 kcal/mol) , while in the case of ^{G40N}CK1α the latter interaction was not affected. In fact, besides ^{N39G}CK1α, the effect of mutations on the CRBN^{His357}–CK1α^{Thr38} interaction was within the estimated uncertainty margins (ΔPMF_{HB_break} of 0.0 ± 0.6, -0.4 ± 0.5 and 1.0 ± 0.5 kcal/mol for the ^{G40N}CK1α, ^{I35G}CK1α and ^{I37E}CK1α mutants respectively). For the ^{I35G}CK1α and ^{I37E}CK1α mutants, only the CRBN^{Asn351} –CK1α^{Ile37} was significantly weakened with respect the *wt* complex, displaying ΔPMF_{HB_break} of 2.5 ± 0.3 kcal/mol and 4.1 ± 0.4 kcal/mol respectively. Therefore, all mutants displayed as or even more robust H–bonds, on average, than the complex between CRBN and CK1α without lenalidomide, but the profile of dissociation energy with respect to the *wt* ternary complex was weakened for at least one of the H–bonds in all the cases.

Table 1. Summary of the absolute and relative PMF_{HB_break} values (in kcal mol^{-1}) for the CRBN– CK1α systems considered in this work. Relative values (in parentheses) are showed with respect to the CRBN–LEN–CK1α complex. Error estimates were obtained by bootstrapping ten times the W profiles used to estimate the PMF.

H–bond (CRBN–CK1α)	**^{wt}CK1α**	**^{wt}CK1α No LEN**	**^{I35G}CK1α**	**^{I37E}CK1α**	**^{N39G}CK1α**	**^{G40N}CK1α**
Trp400–Asn39	10.9 ± 0.3	2.3 ± 0.3 (-8.6 ± 0.6)	10.3 ± 0.3 (-0.6 ± 0.6)	10.7 ± 0.3 (-0.2 ± 0.6)	6.3 ± 0.4 (-4.6 ± 0.7)	-0.4 ± 1.2 (-11.3 ± 1.5)
His357–Thr38	6.2 ± 0.3	3.7 ± 0.6 (-2.5 ± 0.9)	5.8 ± 0.2 (-0.4 ± 0.5)	5.2 ± 0.2 (-1.0 ± 0.5)	4.5 ± 0.1 (-1.7± 0.4)	6.2 ± 0.3 (0.0 ± 0.6)
Asn351–Ile37	10.9 ± 0.1	6.5 ± 0.2 (-4.4 ± 0.3)	8.4 ± 0.2 (-2.5 ± 0.3)	6.8 ± 0.3 (-4.1 ± 0.4)	6.2 ± 0.6 (-4.7 ± 0.7)	5.8 ± 1.0 (-5.1 ± 1.1)
$\sum PMF_{HB\_break}$	28.0 ± 0.7	12.4 ± 1.1 (-15.6 ± 1.8)	24.5 ± 0.7 (-3.5 ± 1.4)	22.7 ± 0.8 (-5.3 ± 1.5)	16.9 ± 1.1 (-11.1 ± 1.8)	12.4 ± 2.4 (-15.6 ± 3.1)

While there is no experimental value that can be linked directly with the calculated ΔPMF_{HB_break} for the breaking of singular H–bonds, we hypothesized that the observed variation in the energy required for breaking the three interactions at the CRBN–CK1α

interface may inform about the stability of the resulting ternary complex with lenalidomide. To probe this possibility, we first established that there was no co–dependence between the breakages of the three hydrogen bonds (Figure S2), and therefore, the energy required to break all three bonds could be approximated as the addition of the individual PMF_{HB_break} values. We found that the sum of PMF_{HB_break} for the three key H–bonds in each of the complexes between CRBN and CK1α was correlated with its estimated binding affinity ($R^2 = 0.94$, Figure 4).

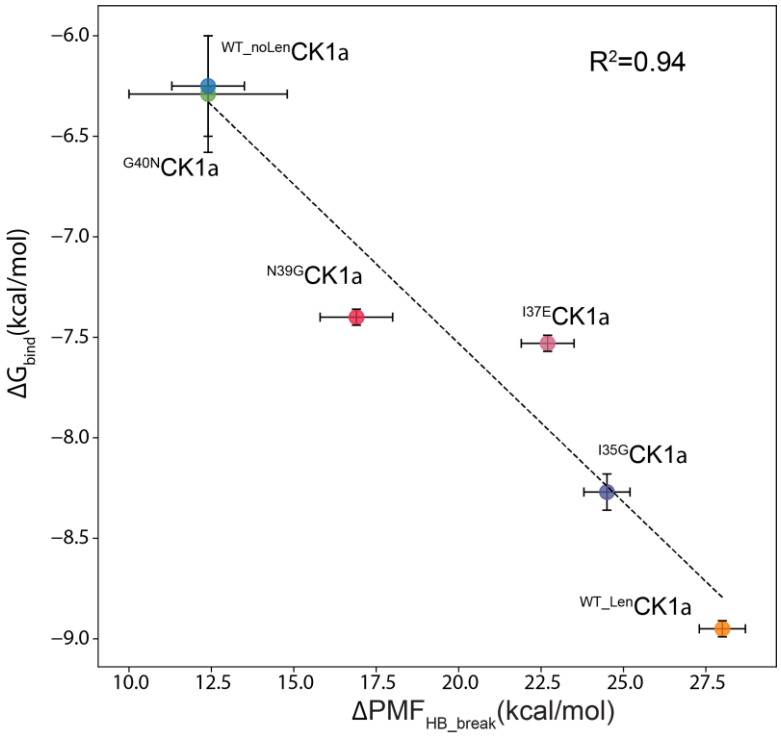

Figure 4: Correlation plot between the sum of the PMF_{HB_break} for the three H–bonds for different variants of CK1α with respect to ΔG_{bin} calculated from K_D estimations. The PMF_{HB_break} was taken at the end point of the PMF profile and error bars were obtained by bootstrapping of the W profiles. PMF_{HB_break} values are reported in table 1. The ΔG_{bin} was obtained by transforming the K_Ds fitted using data from reference[17] and error bars were obtained by error propagation. The reproduced [CRBN]–520/490 nm TR–FRET Ratio plot is provided in supplementary figure S7 and experimental values are provided in supplementary tables S1 and S2.

Weakening of the three H–bond interactions stems from better accessibility of water molecules to the protein–protein interface.

Having stablished the correlation between the strength of the hydrogen bonds at the CRBN–lenalidomide–CK1α interface and the stability of the ternary complex, we next investigated the molecular determinants that could account for the reduced strength of the hydrogen bonds displayed by the four single point CK1α mutants. First, we determined the RDF of water molecules around the H–bonds and compared them with the RDF profiles obtained for the binary and ternary complexes of CK1α (Supplementary Figure S3). All the mutants displayed RDF profiles closer to the ternary complex than to the binary complex. Nevertheless, the profiles obtained for the ternary complex involving the ^{N39G}CK1α mutant was very different that the one obtained for the wild type CK1α, with increased RDF values with respect to the latter in the areas of the first and second solvation shell for both the CRBN^{His357}–CK1α^{Thr38} and the CRBN^{Trp400}–CK1α^{Asn39} H–bonds, while the remaining H–bond (the furthest from the mutation point) only displayed differences beyond 6 Å. A similar pattern was observed on the profiles obtained for the ^{I35G}CK1α and ^{I37E}CK1α mutants, where the closest H–bond was the most affected by the change, although in these cases the differences were only observed on the second solvation shell region. In contrast with the stark decrease in PMF_{HB_break}, the profiles for the remaining mutant ^{G40N}CK1α were indistinguishable from the profiles of the ternary complex with the wild type CK1α. Intrigued by this apparent discrepancy, we visualized the trajectories and identified that, regardless of the system involved, low breaking profiles corresponded with those in which at least one water molecule entered the protein–protein interface from the bulk and established an H–bond with the carbonyl atom previously involved in the protein–protein interaction, while high work profiles corresponded with H–bond breakages in which water molecules did not access the protein–protein interface or did not stablish an H–bond. (Supplementary Movie S1). We hypothesized that the higher rate of access of water molecules to the protein–protein interface in the case of the ^{G40N}CK1α maybe related to a worse hydrophobic packing of lenalidomide's core against the bulkier and more flexible

Asn sidechain than against the Gly residue in position 40. We therefore measured the average distance between lenalidomide's centre of mass and the alpha carbon of residue 40 of CK1α in all the mutants and in the wild type (Figure S4). The average distance was estimated to be ca. 4.8 Å for all the systems but ^{G40N}CK1α, in which the average distance was closer to 5.8 Å.

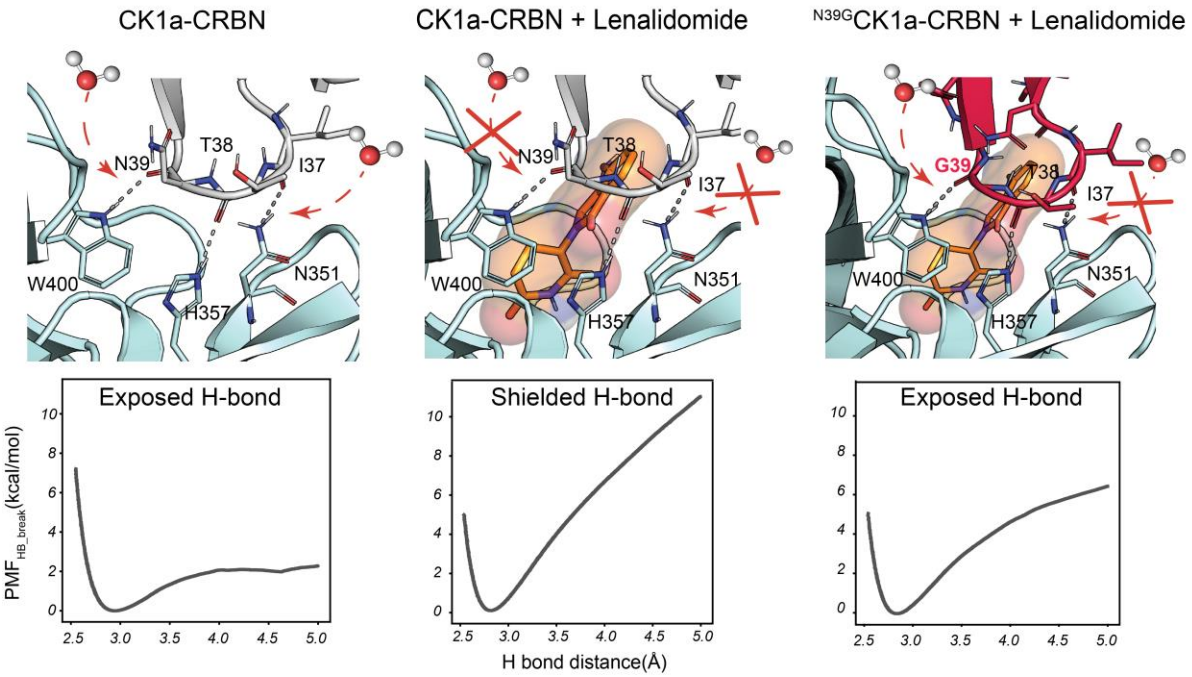

Figure 5: Proposed mechanism underlying the stabilization of the CRBN–CK1α complex by lenalidomide and the effect of mutations in the CK1α sequence. Lenalidomide hinders water accessibility to the CRBN–CK1α interface, increasing the strength of H–bonds. Mutations that alter water accessibility to the interface diminish the stability of the ternary complex.

Considering the results, we propose that lenalidomide (and by extension other IMiDs) enable the degradation of CK1α and other CRBN neo–substrates by strengthening the pre–existing H–bonds at the interface, which results in a complex stable enough as to be tagged by ubiquitination (Figure 5). The reinforcement of the H–bonds seems to be related to the ability of IMiDs to hinder access of water molecules to the protein–protein interface, and hence, their effectiveness is very susceptible to single point mutations that increase the flow of water into the interface, either by means of local or long–range effects.

Discussion

The work demonstrates that the presence of lenalidomide at the CRBN–CK1α interface results in a significant increase in the free energy required to break three key H–bond interactions at the protein–protein interface (Figure 1), as well as highlighting the sensitivity of this effect to point mutations of one of the partners, even when these mutations do not directly hinder the formation of the H–bonds (Figure. 3 and Table 1). Interestingly, we detect an important correlation (squared Pearson R value of 0.94) between the cumulative strength of the three hydrogen bonds and the energy of binding derived from the observed K_D. In principle, there is no reason why the binding energies derived from K_D measurements (an equilibrium property) and the breaking energies of H–bonds (which as computed are an out of equilibrium property) should be correlated. However, we propose that the correlation is not spurious and instead reflects two key mechanistical aspects of the interaction between CRBN and CK1α. First, is that the CK1α point mutations studied are not likely to affect the k_{on} of the complexes, which makes the observed decreases of affinity almost exclusively dependent on changes of the k_{off}. Second, and more crucially, the outstanding correlation between the free energy of H–bonds rupture and the observed affinity indicates that the dissociation of these complexes follows a rather simple two state mechanism, where breaking the H–bonds at the interface is the rate limiting step. Under these circumstances, the PMF_{HB_break} is the major contributor to changes in the $k_{off.}$ And can inform about the equilibrium constant. This observation, together with the dramatic effect of lenalidomide, underscores the potential that rationally designed MGs could hold for the modulation of protein–protein interactions in biomedical and biotechnological settings.

Regarding the underlying mechanism, we have shown that, when bound to the CRBN–CK1α interface, lenalidomide severely hinders water accessibility to the key protein–protein hydrogen bonds, as demonstrated by the stark decrease on the RDF value. (Figure 2) This

hydrophobic shielding effect seems a main driver in the stabilization effect triggered by lenalidomide, and thus could be considered to play a major role in the non–additive effects observed for this compound. It has been previously reported that relatively minor alterations of the H–bond environment can significantly alter H–bond lifetimes.[20,29] This effect is entirely consistent with the stabilization of pre–existing interactions put forward by Cao and co–workers and it is expected that similar mechanism underlies the degradation of other CRBN neo–substrates such as Ikaros and Aiolos and that is shared by other IMiDs such as pomalidomide (Figure 5). Beyond CRBN related systems, by analysing the crystallographic structures available in the PDB, we hypothesize that a similar effect underlies the recently described Cannabidiol–dependent stabilization of a dual–nanobody sensor[19] (PDBid 7TE8) and the long–standing puzzle of the Fucsicoccin–dependent stabilization of interactions involving 14-3-3 proteins (PDBid: 3P1S)[30] (Figure S5). Interestingly, evaluating water accessibility to the protein interface is not enough to anticipate H–bond strength. While the changes triggered by the ^{I35G}CK1α, ^{I37E}CK1α and ^{N39G}CK1α mutations can be rationalised on the basis of local changes to the environment of the H–bond, the behaviour observed for ^{G40N}CK1α is rather unexpected, as an increase in the size and hydrophobicity of the sidechain results in better access of water molecules to the protein–protein interface during the H–bond rupture process, that is not anticipated by RDF profiles of the complexes in equilibrium. Therefore, our results stress that, though often neglected, changes in the protein–protein interactions caused by the presence of MGs are as important as the direc interactions between the MGs and the proteins. We postulate that instead of solely focusing in maximizing affinity, computer–aided drug design strategies for MGs should also aim at maximizing protein–protein interactions by hydrophobic shielding of polar interactions. Analogous strategies should also be investigated for other types of interactions. In this work we demonstrate that an easy–to–implement SMD–based protocol is enough to predict stabilization of H–bonds which, in this

particular system, offer an excellent predictor of the thermodynamic stability of the ternary complex. It remains to be investigated if these results will transfer to other MGs systems, but the incorporation of this strategy in drug design workflows may assist much–needed rational approaches to the design of future MGs

Methods

Molecular simulations setup. Lenalidomide was built using the Molecular Operating Environment software package.[31] Models for the CRBN and CK1α were built starting from the crystallographic structure PDB id. 5FQD,[32] downloaded from the Protein Data Bank.[33–35] Standard protein preparation protocols were followed, including the removal of duplicated proteins, crystallization buffer compounds and salts. Additionally, the DNA Damage–Binding Protein 1 was removed in all systems and the appropriate capping groups were added to the terminal residues of CRBN. Mutants of CK1α were obtained with the mutagenesis wizard tool of PyMOl.[36,37] The ff14SB[38]and gaff2[39] forcefields were used to assign atom types for the protein and the lenalidomide respectively. Partial charges for lenalidomide were derived using the RESP[40,41] protocol at the HF/6-31G(d) level of theory, as calculated with Gaussian09. The Zn^{2+} cation bound to CRBN was modelled using the out of center dummy model[42] Each system, was solvated on a truncated octahedral box of TIP3P[43,44] water molecules and the appropriate number of counterions were added to achieve charge neutrality, accounting for simulations systems of approximately 100000 atoms. Each system was then minimized in three stages: first, the position of water molecules was minimized combining 3500 steps of steepest descent and 6500 steps of conjugate gradient, while the position of the proteins and ligand atoms was restrained using a harmonic potential with force constant of 5.0 kcal mol^{-1} $Å^{-2}$. Next, side chains and water molecules were minimized using 4500 steps of steepest descent, followed by 7500 steps of conjugate gradient while the atoms of lenalidomide and the Zn^{2+} cation were restrained

with a harmonic potential using the same force constant. The systems were then heated in the NVT ensemble from 100 K to 298 K in three stages of 250 ps (100K–150K, 150K–250K, 250K–298K), while retaining the harmonic restraints to lenalidomide and the Zn^{2+} cation and subsequently their density was equilibrated to 1 bar for 1 ns in the NPT ensemble. During the equilibration and subsequent production and steered molecular dynamics trajectories, temperature control was achieved using a Langevin thermostat (with a collision frequency of 3 ps^{-1}) and a Berendesen barostat was used to control the pressure when simulating in the NPT ensemble. SHAKE[45] was applied to all atoms involving hydrogen to allow for a timestep of 2 fs and all simulations were performed with the CUDA accelerated version of PMEMD.[46]

Steered Molecular Dynamics protocol. The stability of each H–bond in each system was assessed using 100 independent SMD trajectories conducted in three stages. First, new velocities were assigned to the equilibrated structure using a different random seed number at 298 K. Subsequently an MD trajectory was performed for 10 ns, using flat–bottom restraints to keep the three protein–protein H–bonds at the interface between 2.5 and 3.5 Å, using a force constant of 60 kcal/mol $Å^2$. Second, the final configuration of each trajectory was then used as a starting structure for a short (1 ns) SMD simulation in which the donor and acceptor involved in one of the H–bonds were brought to a distance of 2.5 Å. Third, a 5 ns–long SMD trajectory was started, in which the distance between donor an acceptor was increased at a rate of 0.5 Å/ns, using a spring constant of 500 kcal/ mol $Å^2$ to ensure the applicability of the stiff spring approximation.[47] The PMF_{HB_break} was then computed leveraging the Jarzynki's equality[48,49] (1).

$$e^{-\Delta G/k_B T} = \langle e^{-W_i/k_B T} \rangle \quad (1)$$

were the right–hand term corresponding to the ensemble average of exponential work values obtained in non–equilibrium conditions. From the above equation, for every increase of 0.0005 Å in the H–bond distance, the PMF_{HB_break} was obtained using expresion (2)

$$PMF_{HB\_break} = -k_B T \, ln \sum_{i=1}^{N} \frac{e^{W_i^{HB\_break}/k_B T}}{N} \quad (2)$$

Where $W_i^{HB\_break}$ refers to the work value of the ith independent SMD trajectory and N is the number of independent SMD trajectories (N=100 in this work). Error estimations for the PMF_{HB_break} profiles were obtained by bootstrapping ten times at each distance point the set of W^{HB_break} values. Convergence of the PMF_{HB_break} at 5 Å of H–bond (Figure S6) distance was evaluated combining subsampling and bootstrapping.

Calculation of water radial distribution function. The radial distribution function of water molecules around the backbone carbonyl oxygen of the CK1α residues involved in the interaction with CRBN was calculated was calculated using cpptraj[50,51], for a range between 0 and 10 Å from the atom of interest and with a bin spacing value of 0.1 Å.

Experimental data sourcing and analysis. Time–resolved fluorescence resonance energy transfer (TR/FRET) data points were extracted from Petzold et. al.[32] using WebPlotDigitizer v4.5[52] and analysis was performed with the Graphpad Prism 8 software.[53] Data points were adjusted to a non–linear regression curve achieving binding saturation. The maximum ratio value obtained for the CRBN–CK1α–lenalidomide ternary complex was use as constrained maximum signal (Ymax) in all the conditions to determine the K_D.

References

1 X. Tan, L. I. A. Calderon-Villalobos, M. Sharon, C. Zheng, C. V Robinson, M. Estelle and N. Zheng, *Nature*, 2007, **446**, 640–645.

2 B. Z. Stanton, E. J. Chory and G. R. Crabtree, *Science (1979)*, , DOI:10.1126/science.aao5902.

3 S. A. Andrei, E. Sijbesma, M. Hann, J. Davis, G. O'Mahony, M. W. D. Perry, A. Karawajczyk, J. Eickhoff, L. Brunsveld, R. G. Doveston, L. G. Milroy and C. Ottmann, *Expert Opin Drug Discov*, 2017, 12, 925–940.

4 L. G. Milroy, T. N. Grossmann, S. Hennig, L. Brunsveld and C. Ottmann, *Chem Rev*, 2014, 114, 4695–4748.

5 Y. Che, A. M. Gilbert, V. Shanmugasundaram and M. C. Noe, *Bioorg Med Chem Lett*, 2018, **28**, 2585–2592.

6 Q. Huai, H.-Y. Kim, Y. Liu, Y. Zhao, A. Mondragon, J. O. Liu and H. Ke, *Proceedings of the National Academy of Sciences*, 2002, **99**, 12037–12042.

7 P. B. Schiff and S. B. Horwitz, *Proceedings of the National Academy of Sciences*, 1980, **77**, 1561–1565.

8 D. E. Bussiere, L. Xie, H. Srinivas, W. Shu, A. Burke, C. Be, J. Zhao, A. Godbole, D. King, R. G. Karki, V. Hornak, F. Xu, J. Cobb, N. Carte, A. O. Frank, A. Frommlet, P. Graff, M. Knapp, A. Fazal, B. Okram, S. Jiang, P.-Y. Michellys, R. Beckwith, H. Voshol, C. Wiesmann, J. M. Solomon and J. Paulk, *Nat Chem Biol*, 2020, **16**, 15–23.

9 M. Słabicki, Z. Kozicka, G. Petzold, Y.-D. Li, M. Manojkumar, R. D. Bunker, K. A. Donovan, Q. L. Sievers, J. Koeppel, D. Suchyta, A. S. Sperling, E. C. Fink, J. A. Gasser, L. R. Wang, S. M. Corsello, R. S. Sellar, M. Jan, D. Gillingham, C. Scholl, S. Fröhling, T. R. Golub, E. S. Fischer, N. H. Thomä and B. L. Ebert, *Nature*, 2020, **585**, 293–297.

10 N. S. Scholes, C. Mayor-Ruiz and G. E. Winter, *Cell Chem Biol*, 2021, **28**, 1048–1060.

11 C. Mayor-Ruiz, S. Bauer, M. Brand, Z. Kozicka, M. Siklos, H. Imrichova, I. H. Kaltheuner, E. Hahn, K. Seiler, A. Koren, G. Petzold, M. Fellner, C. Bock, A. C.

Müller, J. Zuber, M. Geyer, N. H. Thomä, S. Kubicek and G. E. Winter, *Nat Chem Biol*, 2020, **16**, 1199–1207.

12 L. Brunsveld, Y. Higuchi, L.-G. Milroy, S. A. Andrei, C. Ottmann and P. J. de Vink, *Chem Sci*, , DOI:10.1039/c8sc05242e.

13 A. K. Gandhi, J. Kang, C. G. Havens, T. Conklin, Y. Ning, L. Wu, T. Ito, H. Ando, M. F. Waldman, A. Thakurta, A. Klippel, H. Handa, T. O. Daniel, P. H. Schafer and R. Chopra, *Br J Haematol*, 2014, **164**, 811–821.

14 J. Krönke, E. C. Fink, P. W. Hollenbach, K. J. MacBeth, S. N. Hurst, N. D. Udeshi, P. P. Chamberlain, D. R. Mani, H. W. Man, A. K. Gandhi, T. Svinkina, R. K. Schneider, M. McConkey, M. Järås, E. Griffiths, M. Wetzler, L. Bullinger, B. E. Cathers, S. A. Carr, R. Chopra and B. L. Ebert, *Nature*, 2015, **523**, 183–188.

15 E. S. Fischer, K. Böhm, J. R. Lydeard, H. Yang, M. B. Stadler, S. Cavadini, J. Nagel, F. Serluca, V. Acker, G. M. Lingaraju, R. B. Tichkule, M. Schebesta, W. C. Forrester, M. Schirle, U. Hassiepen, J. Ottl, M. Hild, R. E. J. Beckwith, J. W. Harper, J. L. Jenkins and N. H. Thomä, *Nature*, 2014, **512**, 49–53.

16 Q. L. Sievers, G. Petzold, R. D. Bunker, A. Renneville, M. Słabicki, B. J. Liddicoat, W. Abdulrahman, T. Mikkelsen, B. L. Ebert and N. H. Thomä, *Science (1979)*, , DOI:10.1126/science.aat0572.

17 G. Petzold, E. S. Fischer and N. H. Thomä, *Nature*, 2016, **532**, 127–130.

18 M. E. Matyskiela, T. Clayton, X. Zheng, C. Mayne, E. Tran, A. Carpenter, B. Pagarigan, J. McDonald, M. Rolfe, L. G. Hamann, G. Lu and P. P. Chamberlain, *Nat Struct Mol Biol*, 2020, **27**, 319–322.

19 S. Cao, S. Kang, H. Mao, J. Yao, L. Gu and N. Zheng, *Nat Commun*, 2022, **13**, 1–14.

20 P. Schmidtke, F. Javier Luque, J. B. Murray and X. Barril, *J Am Chem Soc*, 2011, **133**, 18903–18910.

21 S. Ruiz-Carmona, P. Schmidtke, F. J. Luque, L. Baker, N. Matassova, B. Davis, S. Roughley, J. Murray, R. Hubbard and X. Barril, *Nat Chem*, 2017, **9**, 201–206.

22 M. Majewski, S. Ruiz-Carmona and X. Barril, *Commun Chem*, 2019, **2**, 110.

23 G. G. Ferenczy and M. Kellermayer, *Comput Struct Biotechnol J*, 2022, **20**, 1946–1956.

24 R. Vogel, M. Mahalingam, S. Lüdeke, T. Huber, F. Siebert and T. P. Sakmar, *J Mol Biol*, 2008, **380**, 648–655.

25 S. Park and K. Schulten, *Journal of Chemical Physics*, 2004, **120**, 5946–5961.

26 H. Xiong, A. Crespo, M. Marti, D. Estrin and A. E. Roitberg, *Theor Chem Acc*, 2006, **116**, 338–346.

27 F. Colizzi, R. Perozzo, L. Scapozza, M. Recanatini and A. Cavalli, *J Am Chem Soc*, 2010, **132**, 7361–7371.

28 R. C. Bernardi, M. C. R. Melo and K. Schulten, *Biochim Biophys Acta*, 2015, **1850**, 872–877.

29 L. M. Nilsson, W. E. Thomas, E. V Sokurenko and V. Vogel, *Structure*, 2008, **16**, 1047–1058.

30 C. Anders, Y. Higuchi, K. Koschinsky, M. Bartel, B. Schumacher, P. Thiel, H. Nitta, R. Preisig-Müller, G. Schlichthörl, V. Renigunta, J. Ohkanda, J. Daut, N. Kato and C. Ottmann, *Chem Biol*, , DOI:10.1016/j.chembiol.2013.03.015.

31 Molecular Operating Environment (MOE), *Scientific Computing & Instrumentation*, 2019, 32.

32 G. Petzold, E. S. Fischer and N. H. Thomä, *Nature*, 2016, **532**, 127–130.

33 H. M. Berman, J. Westbrook, Z. Feng, G. Gilliland, T. N. Bhat, H. Weissig, I. N. Shindyalov and P. E. Bourne, *Nucleic Acids Res*, 2000, 28, 235–242.

34 S. K. Burley, H. M. Berman, C. Christie, J. M. Duarte, Z. Feng, J. Westbrook, J. Young and C. Zardecki, *Protein Science*, 2018, **27**, 316–330.

35 D. S. Goodsell, C. Zardecki, L. Di Costanzo, J. M. Duarte, B. P. Hudson, I. Persikova, J. Segura, C. Shao, M. Voigt, J. D. Westbrook, J. Y. Young and S. K. Burley, *Protein Science*, 2020, 29, 52–65.

36 W. L. Delano, *CCP4 Newsletter on protein crystallography*.

37 W. L. DeLano, *Schrödinger LLC*, 2020.

38 J. A. Maier, C. Martinez, K. Kasavajhala, L. Wickstrom, K. E. Hauser and C. Simmerling, *J Chem Theory Comput*, 2015, **11**, 3696–3713.

39 J. Wang, R. M. Wolf, J. W. Caldwell, P. A. Kollman and D. A. Case, *J Comput Chem*, 2004, **25**, 1157–1174.

40 C. C. I. Bayly, P. Cieplak, W. D. Cornell and P. a Kollman, *J Phys Chem*, 1993, **97**, 10269–10280.

41 T. Fox and P. a. Kollman, *J Phys Chem B*, 1998, **102**, 8070–8079.

42 F. Duarte, P. Bauer, A. Barrozo, B. A. Amrein, M. Purg, J. Åqvist and S. C. L. Kamerlin, *Journal of Physical Chemistry B*, 2014, **118**, 4351–4362.

43 W. L. Jorgensen, J. Chandrasekhar, J. D. Madura, R. W. Impey and M. L. Klein, *J Chem Phys*, 1983, **79**, 926–935.

44 P. Mark and L. Nilsson, *Journal of Physical Chemistry A*, 2001, **105**, 9954–9960.

45 V. Kräutler, W. F. Van Gunsteren and P. H. Hünenberger, *J Comput Chem*, 2001, **22**, 501–508.

46 R. Salomon-Ferrer, A. W. Goetz, D. Poole, S. Le Grand and R. C. Walker, *J Chem Theory Comput*, 2013, **9**, 3878–3888.

47 S. Park, F. Khalili-Araghi, E. Tajkhorshid and K. Schulten, *Journal of Chemical Physics*, , DOI:10.1063/1.1590311.

48 C. Jarzynski, *Phys Rev E Stat Phys Plasmas Fluids Relat Interdiscip Topics*, , DOI:10.1103/PhysRevE.56.5018.

49 C. Jarzynski, *Phys Rev Lett*, , DOI:10.1103/PhysRevLett.78.2690.

50 D. R. Roe and T. E. Cheatham, *J Comput Chem*, , DOI:10.1002/jcc.25382.

51 D. R. Roe and T. E. Cheatham, *J Chem Theory Comput*, , DOI:10.1021/ct400341p.

52 A. Rohatgi, *Pacifica, California, USA*.

53 H. Motulsky, *GraphPad Software Inc*.

AUTHOR INFORMATION

Corresponding Author

* Jordi Juárez-Jimenez – Unitat de Fisicoquímica, Departament de Farmàcia i Tecnologia Farmacéutica, i Fisicoquímica. Facultat de Farmacia I Ciències de l'Alimentació. Universitat de Barcelona (UB). Av. Joan XXIII, 27-31, 08028 Barcelona, Spain.
Email: jordi.juarez@ub.edu

* Xavier Barril – Unitat de Fisicoquímica, Departament de Farmàcia i Tecnologia Farmacéutica, i Fisicoquímica. Facultat de Farmacia I Ciències de l'Alimentació. Universitat de Barcelona (UB). Av. Joan XXIII, 27-31, 08028 Barcelona, Spain.
Email: xbarril@ub.edu

Author Contributions

Marina Miñarro-Lleonar: Investigation, Formal analysis, Software, Visualization, Writing-Review and Editing. **Andrea Bertran-Mostazo:** Investigation, Formal analysis, Writing-Review and Editing. **Jorge Duro:** Investigation. **Xavier Barril:** Conceptualization, Resources, Funding acquisition, Supervision, Writing Review and Editing. **Jordi Juárez-Jiménez:**

Conceptualization, Investigation, Software, Formal analysis, Funding acquisition, Supervision, Project administration, Writing – Original Draft.

ACKNOWLEDGMENT

This work received funding from the research project PDI2020-115683GA-100 ("Proyectos de I+D+i - Modalidad Generación de Conocimiento") financed by MCIN/AEI/10.13039/501100011033 and from the research project RTI2018-096429-N-I00 (Proyectos I+D+i – Modalidad Retos Investigación" financed by MCIN/AEI /10.13039/501100011033/ FEDER "Una manera de hacer Europa". X.B. and J.J-J. are members of the Computational Biology Drug Design Consolidated Research Group supported by the Generalitat de Catalunya (2017SGR1746) A.B-M. is supported by the predoctoral fellowship PRE2019-087468 financed by MCIN/AEI /10.13039/501100011033/ and FSE "El FSE invierte en tu futuro". We thankfully acknowledge access to the Marenostrum 4 HPC facilities granted through the Red Española de Supercomputación (BCV-2019-2-0021 and BCV-2019-3-0012).